International Journal of Academic Engineering Research (IJAER)
ISSN: 2643-9085
Vol. 9 Issue 2 February - 2025, Pages: 41-53

Performance Analysis of Maximum Power Point Tracking Control System for Standalone Photovoltaic Using MRAC Augmented PI Controller

[1]Osinachi Bright Abika, [2]Oliuwafemi Tayo Ojo, [3]Chisom Victory Onyenagubo, [4]Chukwunomso Samuel, [5]Michael Oluwatosin Akinbolusere, [6]Felix Iyanu Ogunleye, [7]Chinonso Valentine Nnachetam

1Electrical and Electronics Engineering, Louisiana Tech University, Louisiana, USA.
Corresponding email address: abikab2022@gmail.com
2Electrical Engineering, Ahmadu Bello University, Zaria 810211, Kaduna State, Nigeria.
3Electrical/Electronic Engineering, Southern University and A&M College 801 Harding Blvd, 70807, Louisiana, USA.
4Electrical/Electronic Engineering, Southern University and A&M College
801 Harding Blvd, 70807, Louisiana, USA.
5Biomedical Technology, Federal University of Technology
PMB 704, Akure, Ondo State, Nigeria.
6Biomedical Technology, Federal University of Technology
PMB 704, Akure, Ondo State, Nigeria.
7Electrical/Electronic Engineering, Southern University and A&M College
801 Harding Blvd, 70807, Louisiana, USA.

Abstract: *The idea behind maximum power point tracking (MPPT) is to ensure that generated power is optimally transferred from the photovoltaic (PV) module to the output of the renewable energy system. Without a proper method to resolve power transfer inefficiency from PV module to connected load, instability may ensue. Hence, in this paper a model reference adaptive control (MRAC) augmented proportional integral (PI) controller called MRAC-PI has been designed to improve the dynamic response characteristics of MPPT control system in a PV system. The system was modelled in MATLAB/Simulink environment. Simulation was initially conducted for the conventional (open loop) MPPT control system and the performance revealed that it suffers from significant overshoot and steady-state error. Hence, the designed MRAC-PI controller was introduced and the adaptation gain selected from low to high value range,* $1 \leq \gamma \leq 30$*.The simulation test revealed that for the adaptation gain considered in this paper the system MRAC-PI provided promising performance and improved stability and reliable control link. An in depth analysis considering the deviation of the system response from the reference model, the update signal, and cost function revealed that with adaptation gain of 15, the system will ensure that efficient and reliable MPPT is achieved with the most optimal model following tracking error. This resulted in rise time of 0.45 s, peak time of 0.91 s, settling time of 1.06, peak overshoot of 2.73%, and zero steady-state error.*

Keywords: Adaptive controller, MPPT, MRAC-PI, PV system, Renewable energy

1. Introduction

Recently, there has been a global move to protect our beloved planet against global warming, which in addition to other causes, owes greatly to greenhouse emission. This move has correspondingly mandated an industrial revolution which has seen an increased level of appreciation and integration of clean energy sources in the industries since the past decade.Solar energy could be one of the significant sources as an alternative energy for the future. In regard to endless importance of solar energy, photovoltaic (PV) energy is considered vital solution for energy crisis. The amount of power generated from any PV panel varies based on the resistive load applied across the panels, and this brings about a reduction in the generated power, even at the same solar irradiance and temperature. Thus, it is imperative to operate PV energy conversion systems in the maximum power-point to maximize the output energy of PV arrays.

The possibility of operatingPVenergyconversionsystemsinthemaximumpowerpoint is not guaranteed if a tracking algorithm is not integrated into the system. Hence the need to integrate a scheme that will ensure that maximum power is extracted from the PV arrays. This scheme is called maximum power point tracking (MPPT) control system. This is usually achieved in PV system by integrating MPPT controller with power electronic converter systems such that the converter's duty cycle is controlled for maximum power transfer to connected load [1,2]. A large number of techniques have been proposed for tracking the maximum power point [3] and they are discussed in the literature. As a result of the various methods implemented for MPPT control system, comparative analysis of different MPPT techniques has been carried out by various researchers. These techniques vary in complexity, cost, convergence speed, sensors required, hardware implementation, and effectiveness.

The control strategy of Perturbation and Observation (P&O) methodinvolvesrepeated perturbing of the voltage of the PV array and then the resulting change in the output power is measured. Though the P&O seems to be a cost effective and quite simple method, it is however not efficient in steady-state since the system must be forced to oscillate about maximum power point (MPP) rather than it being continuously tracked. In addition, under rapidly changing environmental situations, the P&O controller fails due to the fact that it is not able to discern the difference in power changes because of environmental effects against power changes because of perturbation inherently caused by the algorithm[4].This therefore calls for the need to search for other control algorithms that can provide a more efficient result. To this end, this study will examinethe performance of an adaptive integrated with proportional integral controller (MRAC-PI).

2. Literature Review

Some of the studies carried out with respect to MPPT control strategies are concisely presented in this section. The essence of MPPT system is to address the associated solar energy fluctuations through the day. This fluctuation impacts on the output power delivered to load and as such there is need for power correction. Hence, the use fuzzy Type-2 controller for MPPT in full bridge converter on direct current (DC) Nano Grid System in order to track an MPP based on P-V characteristic curve since the PV output power changes with certain conditions such as temperature and irradiation, and as a result brings about unstable output power so that the accuracy of the power generated is not maximum [5].In a dSpace 1104 board, a voltage reference estimator (VRE) that combines the algorithm of fuzzy logic control (FLC) system for maximum power extraction from the PV module was implemented for PEIMAR SD340P, which is a commercial PV module [6]. Two control algorithms, ripple correlation control (RCC) and MRAC, were decoupled to achieve MPPT with more reduced time constants and largely system stability [7,8]. An adaptive P&O algorithm based on short-circuit current concept which consists of two control schemes, specifically,current perturbation algorithm and adaptive control algorithmfor maximum power extraction from PV module considering sudden variations in irradiance was presented [9]. A comparison analysis revealed that linear quadratic regulator (LQR) outperformed classical P&Q algorithm for in a standalone PV unit in providing better MPPT capability [10].

Considering the reviewed literatures, some methods for controlling solar photovoltaic energy system have been reported. These methods are used to establish the algorithm for maximum power point tracking. This paper conductsdynamic response analysis of classical MRAC system and MRAC augmented PI controller.

3. System Design

Figure 1 shows the block diagram of PV system including a DC-DC converter (the power conversion stage), MPPT control system and connected load.In the system, the DC-DC converter is used to facilitate the matching of source and load impedances. This allows maximum power to be transferred from the source to load. Thus, the figure illustrates complete representation of a typical standalone PV system such that the panel impedance is allowed by the MPPT control unit to match with the impedance of the source and thus resulting in the extraction of maximum power. The power stage (boost converter) comprises capacitor, solid state switching device such as MOSFET, inductor, source, and by extension a load. The inductor is placed before the switching device. The PV module is the PV – MLU255HC model and its power rating is 255 W [11,12]. This paper is mainly concerned of with the design of MRAC based technique that basically maximized power from PV system and coordinates the transfer to connected load via DC-DC boost converter. Hence, the DC-DC converter is the plant to be regulated in this case for effective performance and its mathematical modelling will largely covered in this section together with the control systems.

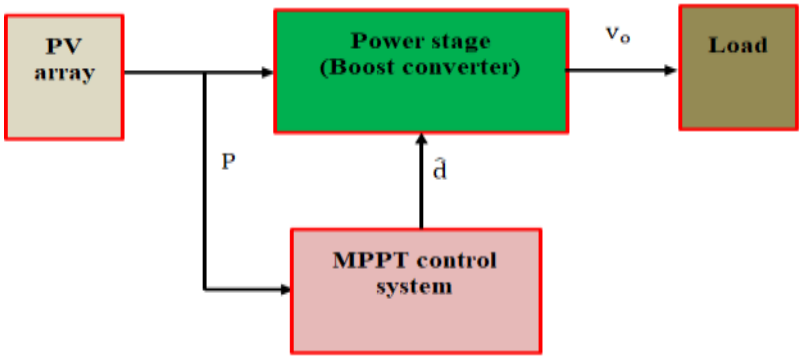

Fig. 1 Block diagram PV system

3.1 Boost Converter Model

In designing a control system for solar PV system, a vital approach is to determine mathematical equations representing the DC-DC converter behaviour as it interfaced the solar panel and the load. The need for modelling is to specifically understand how parameter variations from load voltage, duty cycle, and load current impact on the output voltage. A circuit diagram of boost converter is shown in Fig. 2 to ease the modelling. The following assumptions are made for good design to be achieved: the components are ideal and incurred no loss, operation is in continuous conduction mode covering a time period T wherein switch S_w is closed and opened for periods defined by duty cycle ratio (D) multiplied by time (DT) and $(1-\mathrm{D})$Trespectively, and the fitted capacitor is chosen such that output voltage is constant.

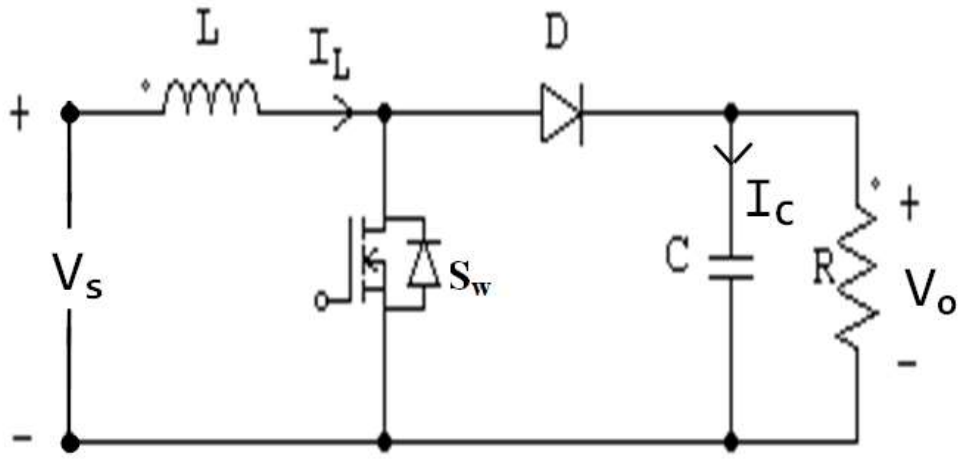

Fig. 2 Boost converter circuit diagram

The operation of a boost converter can be divided into two modes –mode 1 and mode 2 (ON and OFF states). Thus, the modelling in this paper has been performed in this regard. Given the inductor current $I_L$the output voltageV_o, the mathematical definitions for the ON mode and OFF mode are presented in Eq. (1) and (2), respectively.

$$\left.\begin{aligned} \mathrm{L}\frac{\mathrm{di_L}}{\mathrm{dt}} &= \mathrm{v_s} \\ \mathrm{C}\frac{\mathrm{dv_o}}{\mathrm{dt}} &= -\frac{\mathrm{v_o}}{\mathrm{R}} \end{aligned}\right\} \quad \text{where } 0 \le \mathrm{t} < DT\ for\ ON\ mode \tag{1}$$

$$\left.\begin{aligned} \mathrm{L}\frac{\mathrm{dI_L}}{\mathrm{dt}} &= \mathrm{v_s} - \mathrm{v_o} \\ \mathrm{C}\frac{\mathrm{dv_o}}{\mathrm{dt}} &= \mathrm{i_L} - \frac{\mathrm{v_o}}{\mathrm{R}} \end{aligned}\right\} \text{where } \mathrm{DT} \le \mathrm{t} < T\ for\ OFF\ mode \tag{2}$$

where R, L, C are the resistance of the connected load, inductance of the inductor, and capacitance of the capacitor. v_s, i_L,v_o are the source voltage, inductor current, and the output voltage. Now, by multiplying Eq. (1) and (2) with D and $(1-\mathrm{D})$respectively gives:

$$\mathrm{L}\frac{\mathrm{di_L}}{\mathrm{dt}} = \mathrm{Dv_s} + (1-\mathrm{D})(\mathrm{v_s} - \mathrm{v_o}) \Longrightarrow \mathrm{L}\frac{\mathrm{di_L}}{\mathrm{dt}} = \mathrm{v_s} - (1-\mathrm{D})\mathrm{v_o} \tag{3}$$

$$\mathrm{C}\frac{\mathrm{dv_o}}{\mathrm{dt}} = -\mathrm{D}\frac{\mathrm{v_o}}{\mathrm{R}} + (1-\mathrm{D})(\mathrm{i_L} - \frac{\mathrm{v_o}}{\mathrm{R}}) \Longrightarrow \mathrm{C}\frac{\mathrm{dv_o}}{\mathrm{dt}} = (1-\mathrm{D})\mathrm{i_L} - \frac{\mathrm{v_o}}{\mathrm{R}} \tag{4}$$

Considering the equilibrium point $(\hat{\mathrm{i}}_\mathrm{L}, \hat{\mathrm{v}}_\mathrm{o})$, linearizing Eq. (3) and (4) about this point would result in steady-state operating point of the system Eq. (5). This is determined by making the derivative elements in Eq. (3) and (4) zero.

$$\left.\begin{aligned} \hat{\mathrm{v}}_\mathrm{o} &= \frac{\mathrm{v_s}}{(1-\mathrm{D})} \\ \hat{\mathrm{i}}_\mathrm{L} &= \frac{\mathrm{v_s}}{\mathrm{R}(1-\mathrm{D})^2} \end{aligned}\right\} \tag{5}$$

The power converter can be modelled by small signal modelling, which is performed by setting$\mathrm{i_L} = (\mathrm{I_L} + \hat{\mathrm{i}}_\mathrm{L})$, $\mathrm{v_s} = (\mathrm{V_s} + \hat{\mathrm{v}}_\mathrm{s})$, $\mathrm{v_o} = (\mathrm{V_o} + \hat{\mathrm{v}}_\mathrm{o})$, and $\mathrm{D} = (\mathrm{d} + \hat{\mathrm{d}})$in Eq. (3) and (4) gives a linearized equation defined by:

$$\left.\begin{aligned} L\frac{d\hat{i}_L}{dt} &= \hat{v}_s - (1-d)\hat{v}_o + V_o\hat{d} \\ C\frac{d\hat{v}_o}{dt} &= (1-d)\hat{i}_L - \frac{\hat{v}_o}{R} - \hat{i}_L\hat{d} \end{aligned}\right\} \quad (6)$$

Equation (6) can be represented in a state-space canonical form as in [13-16] by letting $\hat{i}_L = x_1, \hat{v}_o = x_2$ given by:

$$\left.\begin{aligned} \dot{x} &= Ax + Bu(t) \\ y &= Cx + D \end{aligned}\right\} \quad (7)$$

Thus, in state-space canonical form as in Eq. (7), Eq. (6) is further expressed as:

$$\left.\begin{aligned} \dot{x} &= \begin{bmatrix} 0 & -\frac{1}{L}(1-d) \\ \frac{1}{C}(1-d) & -\frac{1}{CR} \end{bmatrix} x + \begin{bmatrix} \frac{1}{L} \\ 0 \end{bmatrix}\hat{v}_s + + \begin{bmatrix} \frac{V_o}{L} \\ -\frac{I_L}{C} \end{bmatrix}\hat{d} \\ y &= x_2 = [0 \quad 1]x \end{aligned}\right\} \quad (8)$$

Where $\dot{x} = [\dot{x}_1 \dot{x}_2]^T$ and $x = [x_1 x_2]$. Therefore, Eq. (8) is further expressed as in Eq. (9). The equivalent model of the system in Laplace transform is given by Eq. (10) using $G(s) = C(sI - A)^{-1}B + D$.

$$\left.\begin{aligned} \begin{bmatrix} \dot{x}_1 \\ \dot{x}_2 \end{bmatrix} &= \begin{bmatrix} 0 & -\frac{1}{L}(1-d) \\ \frac{1}{C}(1-d) & -\frac{1}{CR} \end{bmatrix}\begin{bmatrix} x_1 \\ x_2 \end{bmatrix} + \begin{bmatrix} \frac{V_o}{L} & \frac{1}{L} \\ -\frac{I_L}{C} & 0 \end{bmatrix}\begin{bmatrix} \hat{d} \\ \hat{v}_s \end{bmatrix} \\ y &= x_2 = [0 \quad 1]\begin{bmatrix} x_1 \\ x_2 \end{bmatrix} \end{aligned}\right\} \quad (9)$$

$$G(s) = \frac{\hat{V}_o(s)}{\hat{V}_s(s)} = \frac{R(1-D)}{RLCs^2 + Ls + R(1-D)^2} \quad (10)$$

The steady-state operating point of the output voltage is taken as 80V. The numerical values of the system are defined in Table 1. Solving for the load resistance, duty ratio, and the steady-state inductor current gives the expression defined in Eq. (11)-(13). Also, Eq. (14) and (15) were used to determine the inductance and capacitance for the choice of filtering inductor and capacitor. The numerical expression of the transfer function in Eq. (10) is given in Eq. (16).

$$\left.\begin{aligned} P_{max} &= \frac{V_o^2}{R} \\ R &= \frac{V_o^2}{P_{max}} = \frac{80^2}{255} = 25\Omega \end{aligned}\right\} \quad (11)$$

$$D = 1 - \frac{V_{in}}{V_o} = 1 - \frac{31.2}{80} = 0.6 \quad (12)$$

$$I_L = \frac{V_{in}}{R(1-D)^2} = \frac{31.2}{25(0.4)^2} = 7.8A \quad (13)$$

$$L > \frac{(1-D)^2 DR}{2f} = \frac{0.16 \times 0.6 \times 25}{2 \times 20 \times 10^3} = 60\mu H \quad (14)$$

$$C > \frac{DV_o}{V_r Rf} = \frac{0.6 \times 80}{0.02 \times 25 \times 20 \times 10^3} = 4.8mF \quad (15)$$

The numerical expression of G(s) obtained solving Eq. (9) and (10) and subsequently substituting the values of inductance, resistance, capacitor, nominal duty ratio, and switching frequency parameters is given by (Abraham et al., 2023):

$$G(s) = \frac{800000}{s^2 + 963.2s + 768550.4} \quad (16)$$

Table 1: Definition of parameters [11,12]

Description of component	Rating

Input voltage, V_s	$31.2V$
Output capacitance, C	$5.0mF$
Load resistance, R	25.0Ω
Inductance, L	$0.1mH$
Nominal duty ratio, D	0.6
Switching frequency, f_s	$20kHz$

3.2 Design of Control Systems

In this section, a model reference adaptive controller (MRAC) is designed. Many approaches are used in the design such as Lyapunov theory, augmented error theory and Massachusetts Institute of Technology (MIT) rule. In this work, a MRAC is developed using the modified MIT technique as in [17-20]. Designing the MRAC using this approach requires that the error and cost function be established.

a) Adjustment Mechanism

Let the difference between actual output of the DC-DC converter v_o and the reference model output $r_m$be defined as the error, $e_m$given by:

$$e_m = \hat{v}_o - r_m \tag{17}$$

The expression of cost function θaccording to the error in Eq. (17) is written as:

$$J(\theta) = \frac{1}{2}e_m^2 \tag{18}$$

The cost function is minimized in a way that the parameter change is maintained in the path of the negative gradient of J given by:

$$\frac{d\theta}{dt} = -\gamma\frac{\partial J}{\partial \theta} = -\gamma e\frac{\partial e}{\partial \theta} \tag{19}$$

Equation (19) is written as change in θ with respect to time t so as to minimize the cost function to zero. The error e change with θ given as $\partial e/\partial\theta$ is called the sensitivity derivative. The adaptation gain is represented by the quantity γ.

Since the objective is to establish a reference model whose behaviour the plant should follow, this is expressed as:

$$G_m(s) = \delta_o G(s) \tag{20}$$

where$G_m(s)$ and δ_o are the reference model and a parameter with a known value. Equation (20) can be defined by:

$$E_m(s) = \delta G(s)U(s) - \delta_o G(s)U_c(s) \tag{21}$$

where$\delta G(s)U(s) = \hat{V}_o(s)$ and$U(s)$ is the control input, $\delta_o G(s)U_c(s) = R_m(s)$ and $U_c(s)$ is the input to the reference model.

Hence, the control law is defined by:

$$U(s) = \theta U_c(s) \tag{22}$$

With Eq. (22) substituted into Eq. (21) and the partial derivative taken, the following expression is established:

$$\frac{\partial E(s)}{\partial \theta} = \delta G(s)U_c(s) = \frac{\delta}{\delta_o}r_m \tag{23}$$

Substituting Eq. (23) into Eq. (19) gives:

$$\frac{d\theta}{dt} = -\acute{\gamma} e r_m \tag{24}$$

where$\acute{\gamma} = \gamma\frac{\delta}{\delta_o}r_m$ and Eq. (24) stands for the update law for adjusting parameter θ and represents the MRAC adjustment mechanism [17].

b) Reference Model

A reference model of a typical second order system is desired to be generated for the system corresponding to its transfer function in Eq. (16). Thus, for second order system, its canonical form is given by:

$$G_{2nd}(s) = \frac{\omega_n^2}{s^2+2\zeta\omega_n s+\omega_n^2} \tag{25}$$

The reference model transfer function is defined by:

$$G_m(s) = \frac{17.9}{s^2+2.67s+17.9} \tag{26}$$

The overall closed-loop control system for the MRAC-PI controller is shown in Fig. 3, in which the parameters of PI are: $K_p = 0.200$and $K_i = 2.00$.

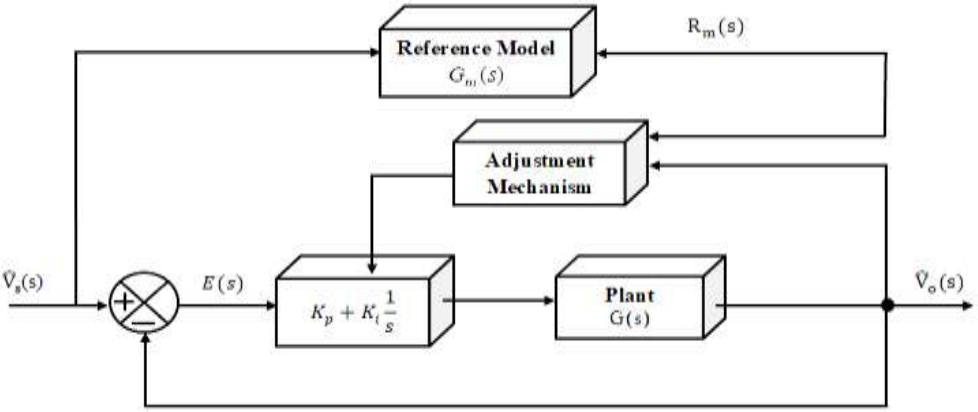

Fig. 3 Block diagram of the MRAC-PI

4. Results and Discussion

In this section, the results from the computer simulation test conducted in MATLAB/Simulink environment are presented. The performance of the MPPT control systemwas initially evaluated in its conventional (open loop) state without a feedback controller as shown in Fig. 4. Then analysis of the designed MPPT control system.

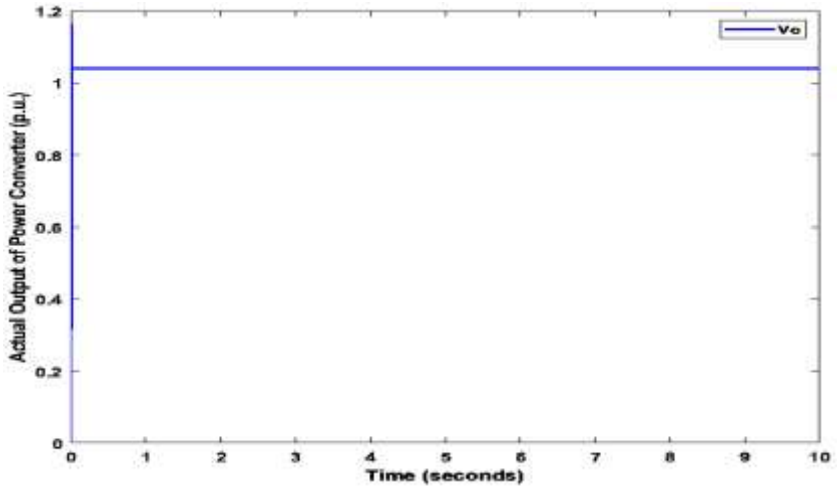

Fig.4 Response of the conventional MPPT control system

The analysis revealed that in this state, the MPPTcontrol system provided the following dynamic response characteristics: rise time of 0.0021 s, settling time of 0.0067 s, overshoot of 11.7%, peak value of 1.1628 p.u., and steady state error of 0.04Ip.u. to unit step input function in p.u. It is evident from Fig. 4that the conventional system was not able to achieve the desired maximum power point tracking and has high overshoot. This indicates that in this state smooth response and reliable MPPT control is not guaranteed because of the associated high overshoot and steady state error above ±0.02 that is usually acceptable for control systems. Thus,

using the system in its conventional state will result in inefficient energy conversion at maximum power point and poor load matching.

The designed controller uses multi-loop strategy to achieve MPPT control. It implements an adaptive mechanism in the outer loop that measures and updates the adjustment parameter according to ensuing error due to the difference between the power converter response and the response of the reference model. The update signal, whose magnitude corresponds to adjustment parameter is use to further fine adjust the PI controller, which provide the inner loop control necessary to adjust the power converter (plant) to desired supply voltage. By this, the system ensured that maximum power (or voltage) is tracked from the sunlight, which is represented as unit step input. Figure 5 shows the response of the MRAC-PI based MPPT control system.

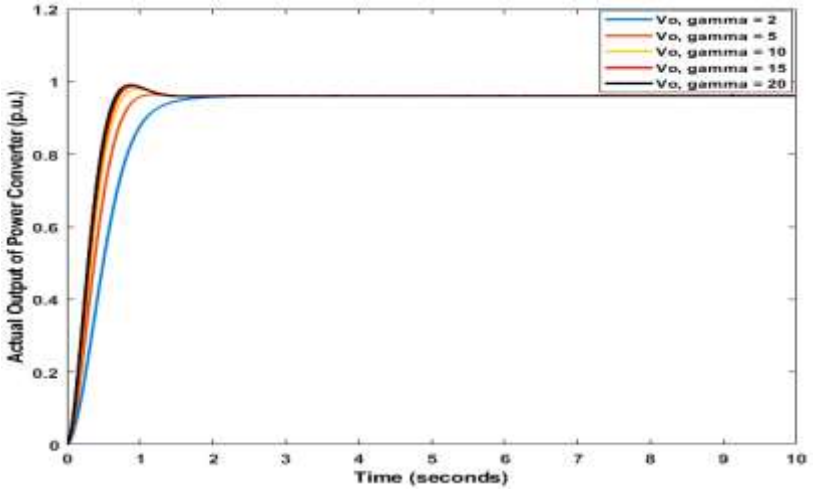

Fig. 5 Voltage output response

In Fig. 5, the response of the designed controller is presented with different curves with respected to varying values of the selected adaptation gains. The selection of the adaptation gain was done by tuning values from low to high and this was used to evaluate the performance of its dynamic or transient response characteristics.The numerical analysis of the MRAC-PI based MPPT control system response is listed in Table 2.Figures 6 to 8 show the simulation plots of the deviation of the actual output from the output of the reference model (e_m), update signal (i.e. whose magnitude corresponds to the adjustment parameterθ, and cost function$J(\theta)$.

Table 2 Dynamic characteristics of the MRAC-PI based MPPT controller

Control state	Rise time (s)	Peak time (s)	Settling time (s)	Peak overshoot (%)	Steady state error
MRAC-PI ($\gamma = 2$)	0.80	8.13	1.41	0	0
MRAC-PI ($\gamma = 5$)	0.57	1.18	0.89	0.39	0
MRAC-PI ($\gamma = 10$)	0.48	0.97	0.72	1.95	0
MRAC-PI ($\gamma = 15$)	0.45	0.91	1.06	2.73	0
MRAC-PI ($\gamma = 20$)	0.43	0.89	1.07	3.34	0

It is evident in Table 2 that the higher the adaptation gain the higher the lower rise time and peak time, but increased peak overshoot. This means that higher value of adaptation results in increase in frequency of oscillation, which causes increased overshoot. Thus, it was observed during simulation tests that after certain values of adaptation gain as it increases, saturation of the output set in. Hence, the analysis of designed MRAC-PI controller was limited to$\gamma = 20$. Generally, the dynamic response characteristics of the system within the range of adaptation seem satisfactorily. The system offered much faster response with$\gamma = 20$. In terms of smooth response, the designed controller provided no oscillation when$\gamma = 2$. In all adaptation gain condition, the controller was able to maintain the desired MPPT with zero steady-state, which means provision of reliable link during tracking of maximum power from sunlight.

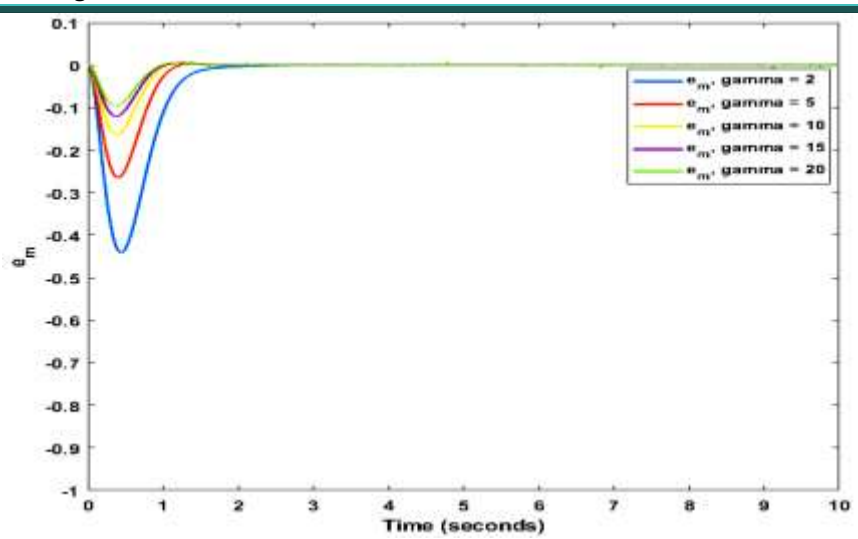

Fig. 6 Error convergence between plant and reference model

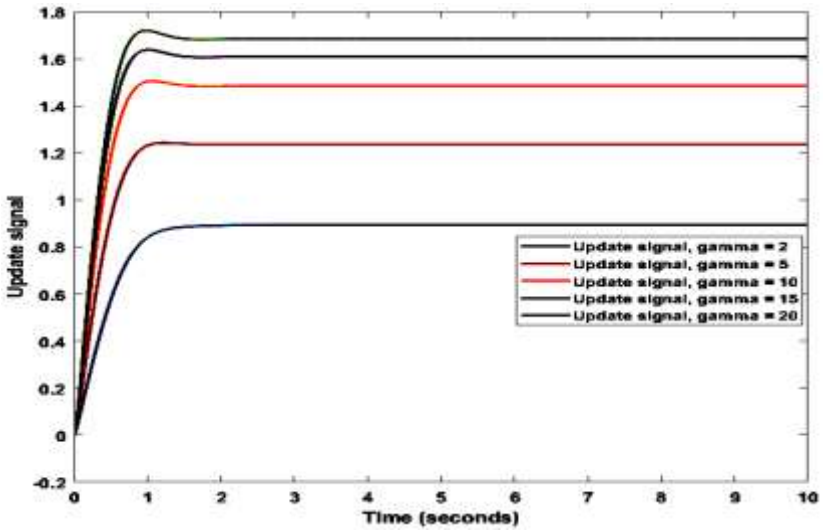

Fig. 7 Adjustment mechanism update signal

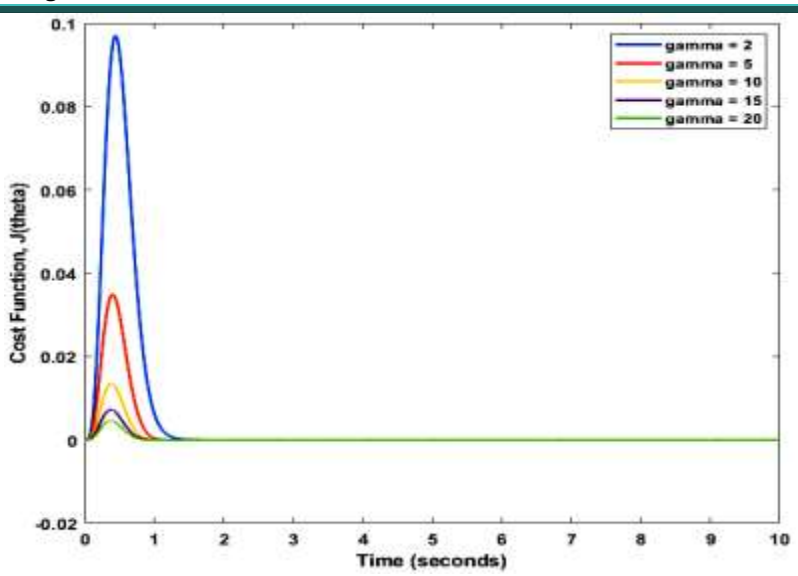

Fig. 8 Cost function curves

Table 3 Numerical performance of the MRAC-PI controller

Control state	e_m	θ	J(θ)
MRAC-PI ($\gamma = 2$)	-5.884e-15	0.8937	1.731e-29
MRAC-PI ($\gamma = 5$)	-8.882e-16	1.238	3.944e-31
MRAC-PI ($\gamma = 10$)	1.11e-15	1.485	6.163e-31
MRAC-PI ($\gamma = 15$)	-4.441e-16	1.609	9.861e-32
MRAC-PI ($\gamma = 20$)	-2.975e-06	1.685	4.424e-12

The numerical analysis of simulation curves in Figures 6 to 8 as listed in Table 3 revealed interesting performances of the controller. It can be seen that the system offered very much reduced deviation of near or equal to zero between the actual output and the reference in all the adaptation gains as shown in Figure 6 and Table 3. In the case of the adjustment parameterθ, it is obvious that increasing γ resulted in increased adjustment force. This means that greater adjustment effort will be required by the outer loop controller to coordinate the action of the inner loop model for effective control action. This causes the control torque ofMRAC-PI to exhibit certain amount of overshoot as the adaptation gain increases. However, with lesser adaptation gain from 1 to 10 the designed system produces a control torque that provides smoother and stable control process. This is obviously by the update signal (adjustment parameter) curves in Figure 7 which looks very much as the response plots of the system in Figure 5. Hence, in implementing the designed MRAC-PI as MPPT controller for PV system, a compromise should be made between lower and higher control torque. For the cost function,J(θ)the objective is to minimize its value for better performance in terms reduced deviation of the power converter plant response from the reference model. This means that a more minimized value ofJ(θ) indicates better following of reference model by the plant and thus improved tracking performance. Thus it suffices to say that the MRAC-PI providedthe finest MPPT for the PV system when $\gamma = 15$ as shown in Figure 8 with $J(\theta) = 9.861e - 32$.

5. Conclusion

In this paper, an adaptive control system based on MRAC augmented PI controller has been designed to provide MPPT for a power converter unit of PV system. The designed controller is a scheme that comprises a PI controller in the inner loop and an MRAC model in the outer loop, which are coupled in a multi-loop control method. The PI parameters were manually determined and the MRAC was developed based on modified MIT rule. The adaptation gain selection was performed by random selection of parameters ranging from low value to higher value. Higher adaptation gain yielded better rise time and peak time, but introduced overshoot with increased adaptation rate. The main reason for this control system is to ensure that a reliable and improved MPPT is achieved for a PV unit and as such, from the analysis, $\gamma = 15$ is recommended as the control condition at which the MRAC-PI will yield the optimal performance in terms of minimized error cost function.

References

[1] Brunton, S. L., Rowley, C. W., Kulkarni, S. R. and Clarkson, C. “Maximum power point tracking for photovoltaic optimization using ripple-based extremum seeking control.” IEEE Trans. Power Electronics.Vol. 25, No.10, pp. 2531–2540, 2010.

[2] Mastromauro, R. A., Liserre, M., Kerekes, T. and Dell'Aquila, A. "A single phase voltage-controlled grid-connected photovoltaic system with power quality conditioner functionality." IEEE Trans. Ind. Electron. Vol. 56, No. 11, pp. 4436–4444, 2009.

[3] Manel, H. and Hfaiedh, M. "Comparison of Different MPPT Algorithms with a Proposed One Using a Power Estimator for Grid Connected PV Systems."*International Journal of Photoenergy.*Hindawi Publishing Corporation. Volume 2016, Article ID 1728398, 10 pages, 2016.http://dx.doi.org/10.1155/2016/1728398.

[4] Jainand, S. and Agarwal, V. "A new algorithm for rapid tracking of approximate maximum power point in photovoltaic systems," IEEE Power Electron. Vol. 2, no. 1, pp. 16–19, 2004.

[5] Prastyawan, A., Efendi, M. and Murdianto, F. "MPPT Full Bridge Converter Using Fuzzy Type-2 on DC Nano Grid System." *Journal on Advanced Research in Electrical Engineering.*Vol. 5, No. 2, pp. 120 – 127, 2021.

[6] Napole, C., Derbeli, M. and Barambones, O. "Fuzzy Logic Approach for Maximum Power Point Tracking Implemented in a Real Time Photovoltaic System," *Journal of Applied Sciences.*Vol. 11, No. 5927 pp. 1 – 18, 2021.https://doi.org/10.3390/app11135927; https://www.mdpi.com/journal/applsci.

[7] Vyshnavi, N. and Subramanian, K. "Model reference adaptive control for maximum power point tracking in PV systems." IJARIIE - ISSN(O) – 2395-4396. Vol-1 Issue-5, pp. 556 – 568, 2015.www.ijariie.com.

[8] Khanna, R., Zhang, Q., Stanchina, W. E., Reed, G. F. and Mao, Z. "Maximum Power Point Tracking Using Model Reference Adaptive Control." IEEE Transactions on Power Electronics.Vol. 29, No. 3, pp. 1490 – 1499, 2014.

[9] Kollimallam, S. K. and Mishra, M. K., (2014). IEEE Transactions on Energy Conversion. pp. 1 – 9, 2014.http://www.ieee.org/publications/standards/publications/rights/index.html.

[10] Anbarasi, M. and Kanthalakshmi, S. (2016). "Linear quadratic optimal control of solar photovoltaic system: An experimental validation." *Journal of Renewable and Sustainable Energy.*Vol. 8.http://dx.doi.org/10.1063/1.4966229.

[11] Abraham, I. I., Mbaocha, C. C., Okozi, S. O., and Benson, M. E. "Maximum power point tracking improvement using incorporated linear quadratic regulator and model reference adaptive control scheme," *Scope*, Vol. 13, No. 4, pp. 1909-1918, 2023.

[12] Abraham, I. I., Mbaocha, C. C., and Okozi, S. O. "Maximum power point tracking improvement using model reference adaptive control scheme," *Science View Journal,* Vol. 4,No. 2, pp. 326-333, 2023. https://doi.org/10.55989/TKOW2858

[13] Eze, P. C., Muoghalu,C. N.,Uebari, B., and C. A. Egbunugha, "State variable feedback control of data centre temperature," *International Journal of Advanced Networking and Applications,* vol. 14, no. 1, pp. 5250-5257, 2022.

[14] Ekengwu, B. O., Eze, P. C., Asiegbu, C. N., Olisa, C. O., and Udechukwu, C. F., "Satellite dish antenna control for distributed mobile telemedicine nodes," *International Journal of Informatics and Communication Technology*, vol. 11, no. 3, pp. 206-217, 2022.

[15] Ekengwu, B. O., Jonathan, A. E., and Eze, P. C., "Effect of control model on internal variable dynamic characteristics of a plant: A state feedback controlled satellite antenna," *International Journal of Academic Multidisciplinary Research,* Vol. 8, No. 3, pp. 163-169, 2024.

[16] Ekengwu, B. O., Eze, P. C., Muoghalu, C. N., Asiegbu, C. N., and Achebe, P. N., "Design of Robust Centralized PID Optimized LQR Controller for Temperature Control in Single-Stage Refrigeration System,"*Indonesian Journal of Electrical Engineering and Informatics*, Vol. 12, No.3, pp. 726-738, 2024. DOI: 10.52549/ijeei.v12i3.5629

[17] Eze, P. C. Njoku, D. O., Nwokonkwo, O. C., Onukwugha, C. G., Odii, J. N., and Jibiri, J. E., "Wheel slip equilibrium point model reference adaptive control based pid controller for antilock braking system: A new approach," *International Journal of Automotive and Mechanical Engineering,* Vol. 21, No. 3, pp. 11581 – 11595, 2024. https://doi.org/10.15282/ijame.21.3.2024.10.0893

[18] Eze, P. C., and Ezenugu, I. A., "Microsatellite yaw-axis attitude control system using model reference adaptive control based PID controller," *International Journal of Electrical Computer Engineering Research,* Vol. 4, pp. 8-16, 2024. https://doi.org/10.53375/ijecer.2024.389

[19] Eze P. C., Jonathan, A. E., Okoronkwo, E. A., and Phillips, A, M. "Improving the transient response performance of CSTR using MRAC," *Iconic Research and Engineering Journals,* Vol. 3, No. 1, pp. 190-196, 2019.

[20] Eze, P. C., Ekengwu, B. O., Muoghalu, C., and Ezeobi, S. O., "Transient response performance improvement of a plastic extrusion process, Elixir Electrical Engineering, 111 (2017) pp. 48717-48721, 2017.

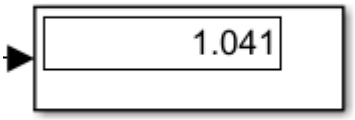

RiseTime: 0.0021
TransientTime: 0.0067

SettlingTime: 0.0067
SettlingMin: 1.0257
SettlingMax: 1.1628
Overshoot: 11.7129
Undershoot: 0
Peak: 1.1628
PeakTime: 0.0048
Y = 2
RiseTime: 0.8022
TransientTime: 1.4126
SettlingTime: 1.4126
SettlingMin: 0.9008
SettlingMax: 1.0000
Overshoot: 1.1149e-08
Undershoot: 0
Peak: 1.0000
PeakTime: 8.1330

Y = 5
RiseTime: 0.5734
TransientTime: 0.8883
SettlingTime: 0.8883
SettlingMin: 0.9006
SettlingMax: 1.0039
Overshoot: 0.3915
Undershoot: 0
Peak: 1.0039
PeakTime: 1.1801

Y = 10
RiseTime: 0.4819
TransientTime: 0.7202
SettlingTime: 0.7202
SettlingMin: 0.9002
SettlingMax: 1.0195
Overshoot: 1.9479
Undershoot: 0
Peak: 1.0195
PeakTime: 0.9690

Y = 15
RiseTime: 0.4469
TransientTime: 1.0643
SettlingTime: 1.0643
SettlingMin: 0.9049
SettlingMax: 1.0273
Overshoot: 2.7333
Undershoot: 0
Peak: 1.0273
PeakTime: 0.9136

Y = 20
RiseTime: 0.4291
TransientTime: 1.0712
SettlingTime: 1.0712
SettlingMin: 0.9009

SettlingMax: 1.0334
Overshoot: 3.3415
Undershoot: 0
Peak: 1.0334
PeakTime: 0.8938

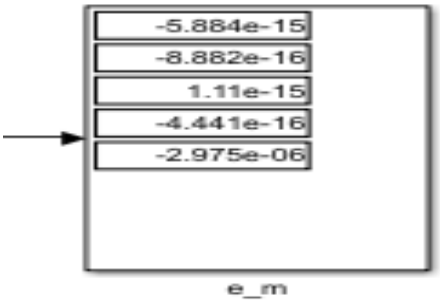

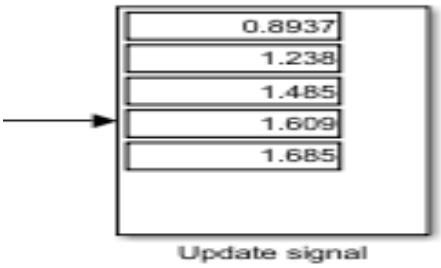

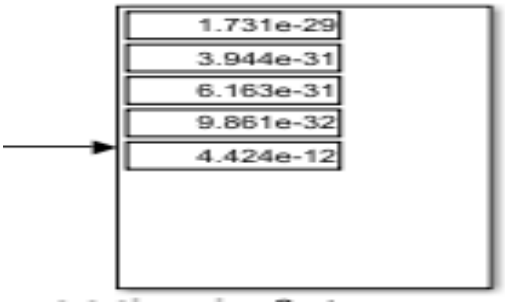

.

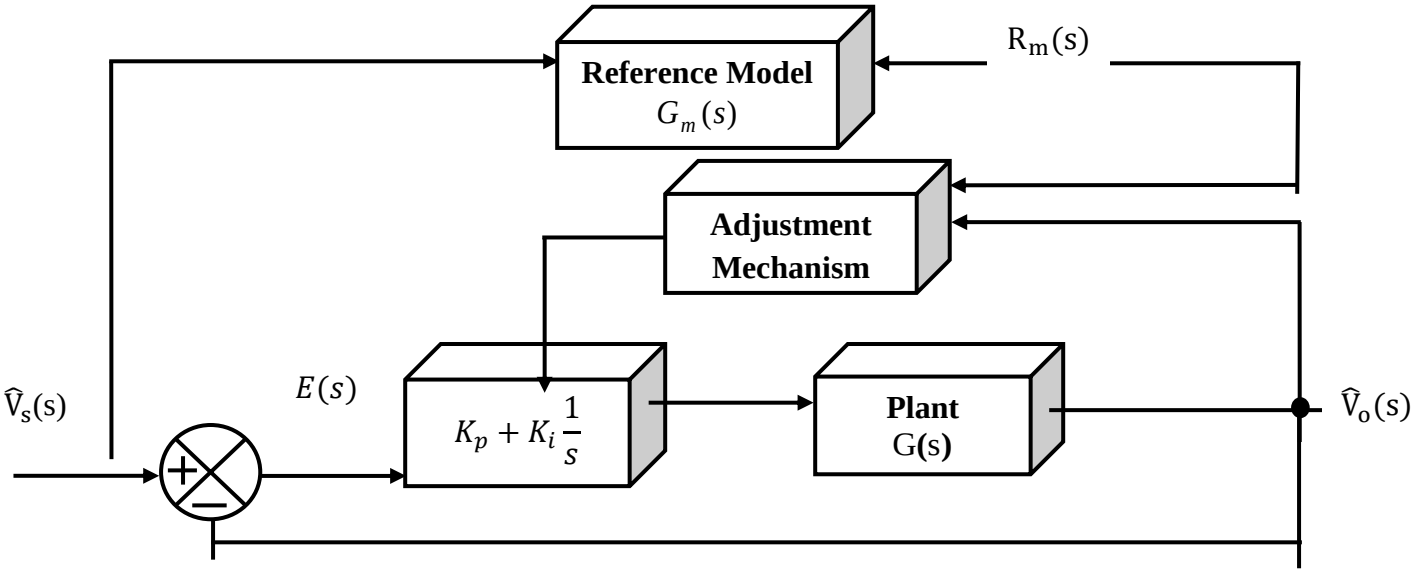

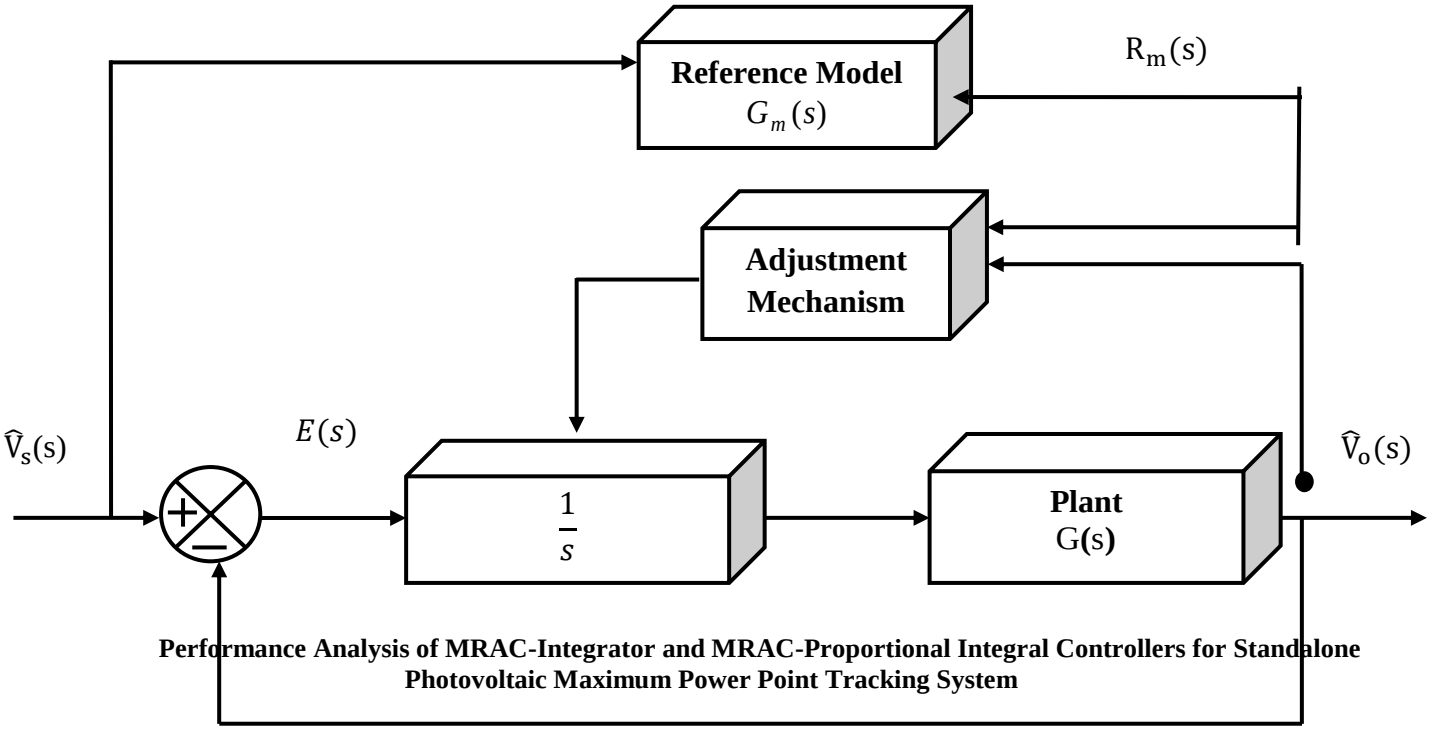

Performance Analysis of MRAC-Integrator and MRAC-Proportional Integral Controllers for Standalone Photovoltaic Maximum Power Point Tracking System